

DSC analysis of Cu–Zn–Sn shape memory alloy fabricated via electrodeposition route

Richard DV. Espiritu · Alberto V. Amorsolo Jr.

Received: 14 January 2011 / Accepted: 7 March 2011 / Published online: 20 March 2011
© Akadémiai Kiadó, Budapest, Hungary 2011

Abstract Cu–Zn–Sn shape memory alloy strips with composition range of 13.70–46.30 mass% Sn were fabricated by electrodepositing Sn on a shim brass surface and then subsequently annealed at a constant temperature of 400 °C for 120 min under flowing nitrogen. Subjecting the Sn-plated strips to differential scanning calorimetry (DSC) analysis revealed that the austenitic start (A_s) temperature was essentially constant at 225 °C while the martensite start (M_s) temperature was consistently within the 221.5–222 °C interval. Austenite to martensite phase transformation showed two distinct peaks on the DSC thermogram which can be attributed to the non-homogeneity of the bulk Cu–Zn–Sn ternary alloy. The latent heats of cooling and heating were found to increase with the mass% Sn plated on the shim brass. Effect of annealing temperature was also investigated wherein strips with an essentially constant composition of 26 mass% Sn were annealed at a temperature range of 350–420 °C for 120 min under flowing nitrogen. Varying the annealing temperature has no significant effect on the transformation temperatures of the ternary alloy.

Keywords Cu–Zn–Sn · Shape memory alloy · Electrodeposition · Phase transformation temperature · Differential scanning calorimetry

Introduction

Shape memory alloys (SMA) are metallic materials that undergo thermoelastic martensitic phase transformation which demonstrates their ability to return to some previously defined shape when subjected to an appropriate thermal procedure. The transformation from one structure to another does not occur by diffusion of atoms but rather by shear lattice distortion [1]. SMAs have remarkable properties such as shape memory effect (SME) and pseudoelasticity which are associated with the specific way the phase transformation occurs. They are being used in various applications which include aircraft hydraulic couplings and electrical connectors, valves in fire-safety devices and implant materials for biomedical applications [2].

Copper-based SMAs are derived from the β -domain of Cu–Zn and Cu–Al systems [3]. Since CuZn-based ternary systems are highly ductile relative to other Cu-based alloys and resist fracture at grain boundaries, they are the only alloys among the Cu-based SMAs exploited for practical application [4]. The Cu–Zn–Sn SMA is of the β -phase type therefore the composition of the resulting ternary alloy should fall within the β -phase region in the phase diagram [5]. By adding a small amount of a ternary element Sn, it is possible to raise the martensitic transformation temperature of binary B2 ordered Cu–Zn [6]. The transformation temperatures of the Cu–Zn–Sn SMA are highly dependent on the amount of metal constituents of the ternary alloy [3].

The differential scanning calorimetry (DSC) analysis is the most widely used technique in determining the phase transformation temperatures and the latent heats due to transformation of SMAs [7–10]. Figure 1 shows a typical DSC plot for SMAs. The martensite start and finish transformation temperatures are typically denoted as M_s and M_f , respectively; the austenite start and finish

R. DV. Espiritu (✉) · A. V. Amorsolo Jr.
Department of Mining, Metallurgical and Materials Engineering,
College of Engineering, University of the Philippines Diliman,
Quezon City 1101, Republic of the Philippines
e-mail: rdvespiritu@up.edu.ph

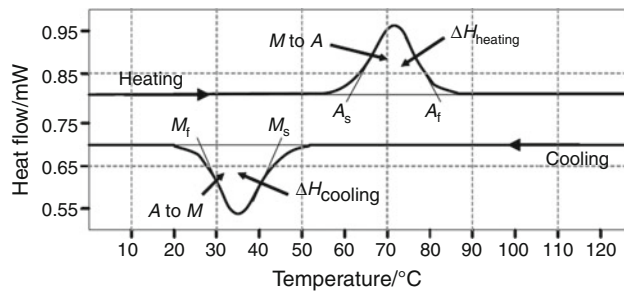


Fig. 1 Typical DSC curve for an SMA showing the transformation temperatures and the latent heat of transformation during heating and cooling [1]

transformation temperatures are denoted as A_s and A_f , respectively. The transformation temperatures from the acquired data are generally measured by drawing tangents to the start and end regions of the transformation peak and the baseline of the heating and cooling curves [1]. Aside from DSC, electrical resistance (ER) measurement was also proven to be effective in determining the phase transformation temperatures of SMA [8].

Though there have been reported studies involving synthesis of SMAs from composite thin films [11] and powders [12–14], there is still no published research involving alternative method via electroplating route which uses the component metal strips as the starting material. Such process offers the advantage of not having a melting step usually used in commercial SMA production. It also avoids the use of expensive forming equipments such as melting furnaces, rolling equipment, or a spin casting facility.

Cu–Zn–Sn SMA fabricated via electrodeposition of tin on brass substrate was successfully synthesized by Espiritu and Amorsolo [15]. Appropriate amount of tin was electrodeposited on a brass substrate and was then subsequently annealed. The scanning electron micrograph of the Cu–Zn–Sn SMA using backscattered electron imaging is shown in Fig. 2. SEM analysis showed the presence of intermetallic layers and probing using EDX analysis revealed that the intermetallic layer produced adjacent to the unreacted brass has an average composition in terms of atomic percent of 57.20, 33.96, and 8.84% for Cu, Zn, and Sn, respectively, as shown in Table 1. This is consistent with reported literature values for composition of Cu–Zn–Sn alloys which is attributed to the layer that exhibits SME. Probe points 1 and 3 correspond to the Cu–Zn–Sn intermetallic layer while probe point 2 corresponds to the unreacted shim brass substrate.

Due to the limited literature available on thermal analysis of Cu–Zn–Sn SMA fabricated by electrodeposition, this research focuses on the determination of the phase transformation temperatures and latent heats of transformation of the fabricated Cu–Zn–Sn SMA by electrodeposition of tin on shim brass.

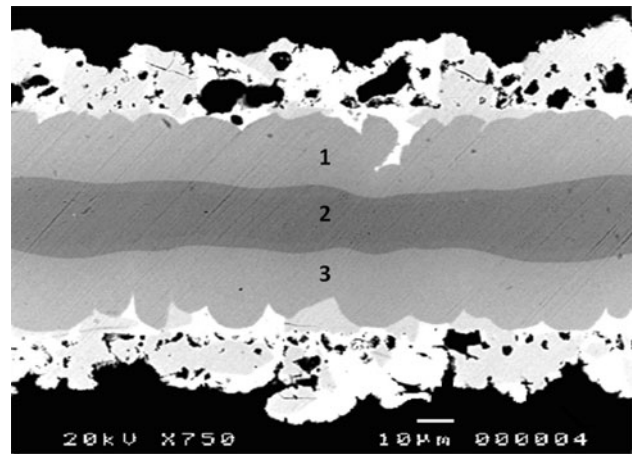


Fig. 2 Scanning electron micrograph of Sn-brass strip annealed at 420 °C [15]

Table 1 EDX elemental composition of the unreacted brass and the adjacent intermetallic layers

Position	Atomic percent		
	Cu	Zn	Sn
1	57.02	32.65	10.33
2	63.34	36.58	0.08
3	57.39	35.26	7.34

Experimental method

Specimen preparation

Commercial shim brass which was procured from a local automobile parts shop was cut to 8 × 2 cm strips using a paper cutter. The strip was then polished using sandpaper Grit 400 for 200 strokes on each side under running water. This was done to remove the dirt and residues on the brass surface and to ensure optimum coating during DC tin plating.

The sulfuric acid–sulfate plating bath was prepared with the following components, namely, 45 g/L stannous sulfate, 150 g/L sulfuric acid, and 2 g gelatin. Pure tin (99.85% purity) was used as the anode and the polished shim brass served as the cathode and were positioned 2 cm apart both immersed into the prepared plating bath. Plating commenced immediately after setting the current to 20 mA. When half of the computed plating time for one side had elapsed, the brass was turned over to electrodeposit the other side until the next half of the computed plating time was reached.

After the desired amount of tin was electrodeposited on both surfaces of the brass substrate, the tin-plated strip was extracted from the bath and was washed with running water. To anneal, the Sn-plated strip was placed standing

laterally in an alumina boat and then fed in the middle of a Carbolite MTF 12/38/250 High Temperature Tube Furnace under flowing nitrogen. The ramping rate for all runs was set to 50 °C/min and annealing temperatures were set to 350, 380, 400, and 420 °C. After annealing, the metal strip was immediately removed from the tube furnace and quenched in ice-water bath.

DSC analysis

Portions of each sample with uniform diameter of 3 mm were prepared using Gatan Disc Punch Model 659 and were subsequently subjected to DSC Analysis. The test was performed using TA Instruments DSC Q10 wherein cell calibration was performed using Indium standard. Each sample was subjected to temperature scan range of 0–400 °C with both cooling and heating profile. The heating curve was obtained by heating the sample hermetically up to 400 °C at 5 °C/min ramp rate followed by cooling down to 30 °C at 3 °C/min rate to obtain the cooling curve. The initial shim brass was also subjected to the same thermal analysis. The obtained data were processed using TA Universal Analysis 2000 software.

Results and discussion

DSC analysis of shim brass substrate

Binary Cu–Zn alloy was also reported to exhibit SME at a particular composition of Cu and Zn [16]. SEM–EDX analysis, Fig. 2, as indicated in Table 1 shows that the initial composition of the brass substrate is 63.4 at% Cu and 36.6 at% Zn. With this composition in the Cu–Zn phase diagram, the shim brass substrate has an $\alpha + \beta'$ phase composition at room temperature.

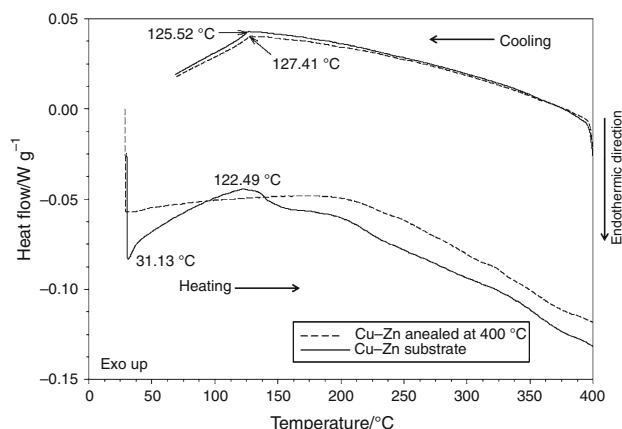


Fig. 3 The DSC thermogram of shim brass and annealed shim brass at 400 °C

The initial shim brass and annealed shim brass were subjected to DSC analysis to verify whether the substrate has innate shape memory properties. Based on Fig. 3, the shim brass substrate did not show any characteristic transformation temperature typical for SMAs reported in literature [16]. Therefore, the DSC thermogram confirms that the shim brass substrate has no innate shape memory properties.

The peak observed at 122.49 °C can be due to the recrystallization of brass brought about by cold work or deformation processes that the shim brass has undergone. On the other hand, the exothermic peaks observed can be attributed to the β' phase formation brought about by cooling from purely α phase region to attain the $\alpha + \beta'$ phase composition of shim brass at room temperature.

DSC analysis of Cu–Zn–Sn SMA with increasing mass% Sn

The superimposed DSC heating and cooling curves of the annealed Sn-brass strips from the lowest to the highest mass% Sn are shown in Figs. 4 and 5, respectively. The endothermic peaks as shown in Fig. 4 appear to be essentially constant at 225 °C. Such endothermic peaks in the annealed samples are attributed to the martensite to austenite transformation due to the presence of intermetallic phases in the alloy. The endothermic peak from the heating curve of annealed samples is the austenite transformation temperature while the exothermic peak from the cooling curve is interpreted as the martensite transformation temperature. Also, it can be observed from Fig. 5, some cooling curves show two exothermic peaks. On the other hand, the heating curve of annealed Sn-brass strip with 46.30 mass% Sn composition also exhibits more than one endothermic peak as shown in Fig. 4. These peaks can be due to the non-homogeneity of the bulk ternary alloy since there is still an unreacted Sn layer on the surface.

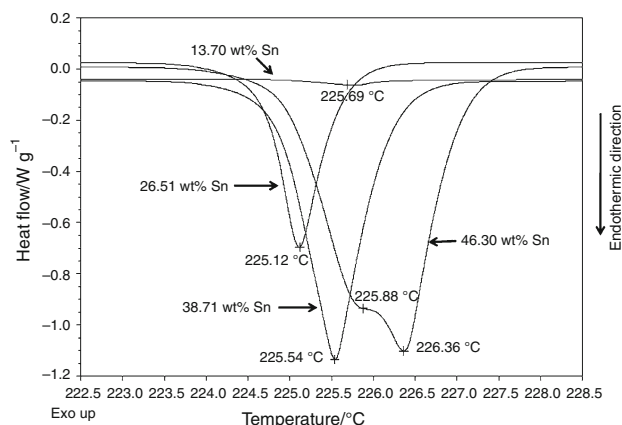


Fig. 4 Superimposed DSC heating curves for annealed samples in terms of increasing mass% Sn

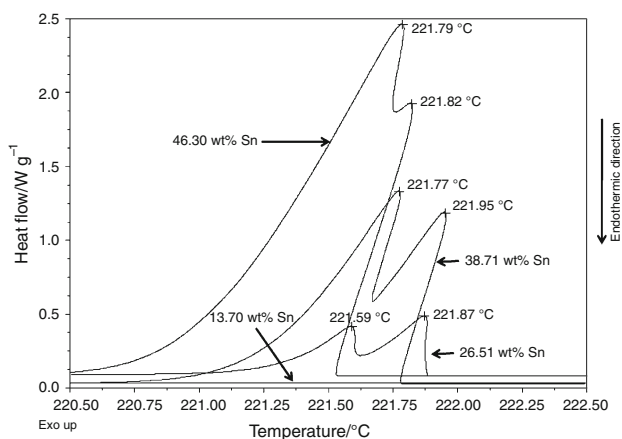


Fig. 5 Superimposed DSC cooling curves for annealed samples in terms of increasing mass% Sn

The results of the DSC analysis in terms of increasing mass% Sn are summarized in Table 2. It can be observed that each characteristic transformation temperature is essentially constant for all annealed Sn-plated brass strips. Since the transformation temperatures are greatly dependent on the composition [9], it is therefore deduced that the resulting ternary alloy corresponding to the intermetallic layer has essentially consistent percent composition of the three metal constituents regardless of the amount of the Sn electrodeposited on the surface.

During the transformation, a latent heat associated with the transformation is absorbed or released based on the transformation direction. The martensite-to-austenite ($M \rightarrow A$) transformation is an endothermic phase transformation accompanied by absorption of thermal energy. On the other hand, the austenite-to-martensite ($A \rightarrow M$) transformation is accompanied by the release of heat corresponding to a change in the transformation enthalpy or exothermic phase transformation [3].

It can also be observed that as the mass% Sn increases for annealed samples, the ΔH of heating and ΔH of cooling also increases. The increasing amount of Sn generally increases the thickness of the intermetallic layer. This therefore translates to the presence of more parent phases, requiring higher amount of energy to completely transform all these parent phases to martensite phases. This can also be attributed to the increased amount of Sn on the surface which causes the ΔH of reaction to increase.

Effect of annealing temperature

This study also investigated the effect of annealing temperature on the transformation temperatures and to the energies of transformation. DSC cooling and heating curves for varying annealing temperatures namely, 350, 380, 400, and 420 °C are shown in Figs. 6 and 7, respectively. The obtained data are summarized in Table 3.

The DSC plots revealed that the transformation temperatures are essentially consistent regardless of the

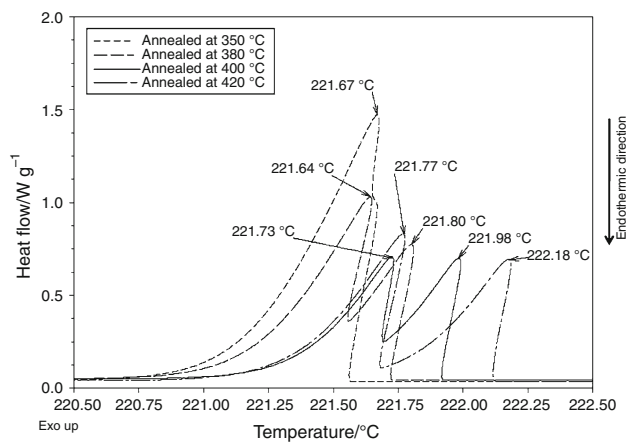


Fig. 6 Superimposed DSC cooling curves for varying annealing temperatures

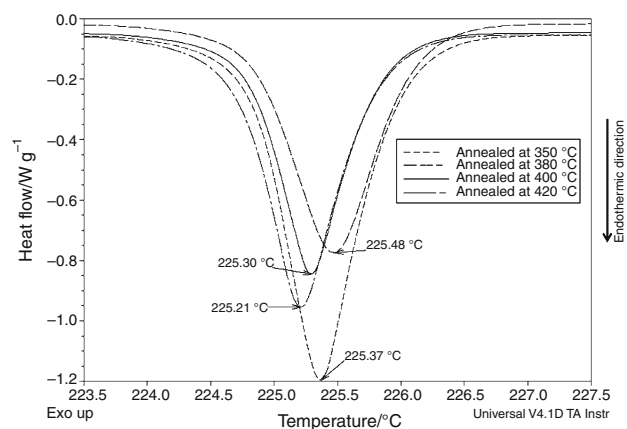


Fig. 7 Superimposed DSC heating curves for varying annealing temperatures

Table 2 Data for transformation temperatures and energy of transformation for annealed samples with increasing weight percent tin

Mass% tin	$A_s/^\circ\text{C}$	$A_f/^\circ\text{C}$	$M_s/^\circ\text{C}$	$M_f/^\circ\text{C}$	ΔH heating/ J g^{-1}	ΔH cooling/ J g^{-1}
13.70	225.01	226.11	–	–	0.1858	–
26.51	224.65	225.63	221.88	221.47	5.879	2.66
38.71	224.85	226.16	221.78	221.25	11.00	9.398
46.30	225.01	226.97	221.55	221.03	17.72	17.57

Table 3 Data for transformation temperatures and energy of transformation for samples annealed at varying temperature

Annealing temperature/°C	A_s /°C	A_f /°C	M_s /°C	M_f /°C	ΔH heating/J g ⁻¹	ΔH cooling/J g ⁻¹
350	224.82	225.96	221.56	221.17	10.46	7.616
380	224.83	226.09	221.74	221.21	7.698	6.267
400	224.77	225.85	221.92	221.48	6.858	4.739
420	224.67	225.82	222.13	221.37	8.415	5.977

annealing temperature employed. For annealing temperature above 350 °C, the cooling curves exhibit two exothermic peaks. Since the transformation temperatures are essentially consistent with one another, it is safe to conclude that the compositions of the intermetallic product layer in the ternary alloys are basically constant regardless of the annealing temperature employed. The figures show noticeable trend of decreasing energies of transformation both for the heating and cooling curves but the disparity between the ΔH values is not appreciably significant. The disparity between the ΔH values for all the annealed runs can be attributed to the amount of unreacted Sn present on the surface of the ternary alloy.

Conclusions

The DSC analysis revealed that the obtained austenite start (A_s) temperature appeared to be essentially constant at 225 °C while the martensite start (M_s) temperature was consistently within the 221.5–222 °C interval. It was also observed that as the mass% Sn increases, the ΔH of heating and ΔH of cooling also increase. Phase transformation from austenite to martensite showed two distinct peaks on the DSC plot which can be due to non-homogeneity of the bulk ternary alloy evinced by the presence of unreacted Sn layer on the surface. Varying the annealing temperature has no significant effect on the transformation temperatures of the Cu–Zn–Sn SMA.

Acknowledgements This research was funded by the Philippine Council for Advanced Science and Technology Research and Development (PCASTRD) of the Department of Science and Technology (DOST).

References

- Lagoudas DC, editor. Shape memory alloys: modeling and engineering applications. New York: Springer; 2008.
- Schwartz M. New materials processes and methods technology. FL: CRC Press Taylor & Francis Group, LLC; 2006.
- Patoor E, et al. Shape memory alloys, part I: general properties and modeling of single crystals. *Mech Mater.* 2006;38:391–429.
- Funakubo H, editor. Shape memory alloys. New York: Gordon and Breach Science Publishers; 1984.
- Tadaki T, Otsuka K, Shimizu K. Shape memory alloys. *Annu Rev Mater Sci.* 1988;18:25–45.
- Castro Riglos M, Pelegrina J, Ahlers M. Phase stability in Cu–Zn based ternary alloys with elements of column 14. *Mat Sci Eng A.* 2008;481–482:504–8.
- Uchil J. Shape memory alloys—characterization techniques. *Pramana J Phys.* 2002;58(5):1131–9.
- Nespoli A, Besseghini S. A complete thermo-mechanical study of a NiTiCu shape memory alloy wire. *J Therm Anal Calorim.* 2010; doi:10.1007/s10973-010-1042-z.
- Coll R, et al. Martensitic transformation in Mn–Ni–Sn Heusler alloys. *J Therm Anal Calorim.* 2010;99:905–9.
- Petalis P, Makris N, Psarras GC. Investigation of the phase transformation behaviour of constrained shape memory alloy wires. *J Therm Anal Calorim.* 2006;1:219–24.
- Tomozawa M, Kim HY, Miyazaki S. Microactuators using R-phase transformation of sputter-deposited Ti-47.3 Ni shape memory alloy thin films. *J Intel Mat Syst Str.* 2006;17:121049–58.
- Eisenwasser JD, Brown LC. Pseudoelasticity and the strain-memory effect in Cu–Zn–Sn alloys. *Metall Trans.* 1972;3:1359–63.
- Hsu C, et al. The precipitation behavior of α_1 -plate and γ phase in Cu–Zn–Sn shape memory alloy. *Mater Trans.* 2006;47(9):2427–33.
- Frackowiak JE, Morgiel J, Dutkiewicz J. Study of the ageing effects on the structure of CuZnSn shape memory alloy. *Hyperfine Interact.* 1986;28:1063–6.
- Espiritu R, Amorsolo A. SEM–EDX analysis of intermetallic phases in a Cu–Zn–Sn shape memory alloy. *Microsc Anal.* 2010;24(6):15–7 (AM).
- Miyazaki S, Otsuka K. Development of shape memory alloys. *J Iron Steel Res Inst.* 1989;29(5):353–77.